JCI The Journal of Clinical Investigation

Podocyte-specific RAP1GAP expression contributes to focal segmental glomerulosclerosis–associated glomerular injury

Uma Potla, … , Paul E. Klotman, Lewis Kaufman

J Clin Invest. 2014;124(4):1757-1769. https://doi.org/10.1172/JCI67846.

Research Article

Injury to the specialized epithelial cells of the glomerulus (podocytes) underlies the pathogenesis of all forms of proteinuric kidney disease; however, the specific genetic changes that mediate podocyte dysfunction after injury are not fully understood. Here, we performed a large-scale insertional mutagenic screen of injury-resistant podocytes isolated from mice and found that increased expression of the gene *Rap1gap*, encoding a RAP1 activation inhibitor, ameliorated podocyte injury resistance. Furthermore, injured podocytes in murine models of disease and kidney biopsies from glomerulosclerosis patients exhibited increased RAP1GAP, resulting in diminished glomerular RAP1 activation. In mouse models, podocyte-specific inactivation of *Rap1a* and *Rap1b* induced massive glomerulosclerosis and premature death. Podocyte-specific *Rap1a* and *Rap1b* haploinsufficiency also resulted in severe podocyte damage, including features of podocyte detachment. Over-expression of RAP1GAP in cultured podocytes induced loss of activated β1 integrin, which was similarly observed in kidney biopsies from patients. Furthermore, preventing elevation of RAP1GAP levels in injured podocytes maintained β1 integrin–mediated adhesion and prevented cellular detachment. Taken together, our findings suggest that increased podocyte expression of RAP1GAP contributes directly to podocyte dysfunction by a mechanism that involves loss of RAP1-mediated activation of β1 integrin.

Podocyte-specific RAP1GAP expression contributes to focal segmental glomerulosclerosis–associated glomerular injury

Uma Potla,[1] Jie Ni,[1] Justin Vadaparampil,[1] Guozhe Yang,[1,2] Jeremy S. Leventhal,[1,2] Kirk N. Campbell,[1] Peter Y. Chuang,[1] Alexei Morozov,[3] John C. He,[1,2] Vivette D. D'Agati,[4] Paul E. Klotman,[5] and Lewis Kaufman[1,2]

[1]Division of Nephrology, Icahn School of Medicine at Mount Sinai, New York, New York, USA. [2]Renal Section, James J. Peters Veterans Affairs Medical Center, New York, New York, USA. [3]Virginia Tech Carilion Research Institute, Roanake, Virginia, USA. [4]Department of Pathology, Columbia University Medical Center, New York, New York, USA. [5]Baylor College of Medicine, Houston, Texas, USA.

Injury to the specialized epithelial cells of the glomerulus (podocytes) underlies the pathogenesis of all forms of proteinuric kidney disease; however, the specific genetic changes that mediate podocyte dysfunction after injury are not fully understood. Here, we performed a large-scale insertional mutagenic screen of injury-resistant podocytes isolated from mice and found that increased expression of the gene *Rap1gap*, encoding a RAP1 activation inhibitor, ameliorated podocyte injury resistance. Furthermore, injured podocytes in murine models of disease and kidney biopsies from glomerulosclerosis patients exhibited increased RAP1GAP, resulting in diminished glomerular RAP1 activation. In mouse models, podocyte-specific inactivation of *Rap1a* and *Rap1b* induced massive glomerulosclerosis and premature death. Podocyte-specific *Rap1a* and *Rap1b* haploinsufficiency also resulted in severe podocyte damage, including features of podocyte detachment. Over-expression of RAP1GAP in cultured podocytes induced loss of activated β1 integrin, which was similarly observed in kidney biopsies from patients. Furthermore, preventing elevation of RAP1GAP levels in injured podocytes maintained β1 integrin–mediated adhesion and prevented cellular detachment. Taken together, our findings suggest that increased podocyte expression of RAP1GAP contributes directly to podocyte dysfunction by a mechanism that involves loss of RAP1-mediated activation of β1 integrin.

Introduction

Podocytes, the terminally differentiated visceral epithelial cells of the glomerulus, are responsible for forming and regulating the kidney filtration barrier. These cells have a remarkably complex cellular morphology, extending numerous interdigitating foot processes that surround the glomerular capillary walls and form unique specialized intercellular junctions known as slit diaphragms. The importance of slit diaphragms is enforced by the abundance of glomerular disorders that are caused by mutations in genes that encode components of this complex. A podocyte's intricate shape is maintained by a well-organized and dynamic actin cytoskeleton that is tightly regulated. In all forms of human proteinuric kidney disease, the podocyte undergoes cytoskeletal remodeling that results in foot process effacement and loss of normal filtration barrier selectivity, a process that is common to nearly all forms of podocyte injury, regardless of the underlying cause (1). The molecular mechanisms driving foot process effacement versus recovery are only beginning to be understood and are paramount to the identification of novel therapeutic strategies for proteinuria.

The original goals of our studies were not only to identify pathways that are dysregulated in podocytes in response to injury, but also to select for those pathways that have the largest functional impact when dysregulated. To accomplish this, we designed and performed a novel large-scale mutagenic screen of genetically resistant podocytes that identified specific chromosomal loci based on whether an insertional mutation at that locus was sufficient to overcome resistance and allow for injury. We found that an insertional mutation in the genetic locus *Rap1gap* resulted in dramatically increased *Rap1gap* transcription and was sufficient to allow genetically resistant HIV-infected podocytes to demonstrate anchorage-independent growth. RAP1GAP is known in other cell types to be an important negative regulator of the small GTPase RAP1, which is involved in diverse biological functions, including polarity, adhesion, cell-matrix interactions, and actin cytoskeletal remodeling (2). RAP1 can be activated by a variety of extracellular signals, which induce the conversion of the inactive, GDP-bound form into the active, GTP-bound form. Cellular RAP1 activity is tightly regulated by a series of guanine nucleotide exchange factors (GEFs) that activate RAP1 and RAP1-specific GTPase–activating proteins (RAPGAPs), including RAP1GAP, that inactivate RAP1 (3). Expression levels of RAP1GAP are dramatically diminished in human epithelial malignancies, including colon (4), thyroid (5), melanoma (6), and others, through a mechanism partially involving promoter methylation. The significance of RAP1 signaling pathways in podocytes, however, is unknown.

Our further studies established that increased podocyte RAP1GAP expression levels represented a critical contributor to podocyte dysfunction after injury. We demonstrated that RAP1GAP expression levels in podocytes were dramatically increased both

Conflict of interest: The authors have declared that no conflict of interest exists.
Citation for this article: *J Clin Invest.* 2014;124(4):1757–1769. doi:10.1172/JCI67846.

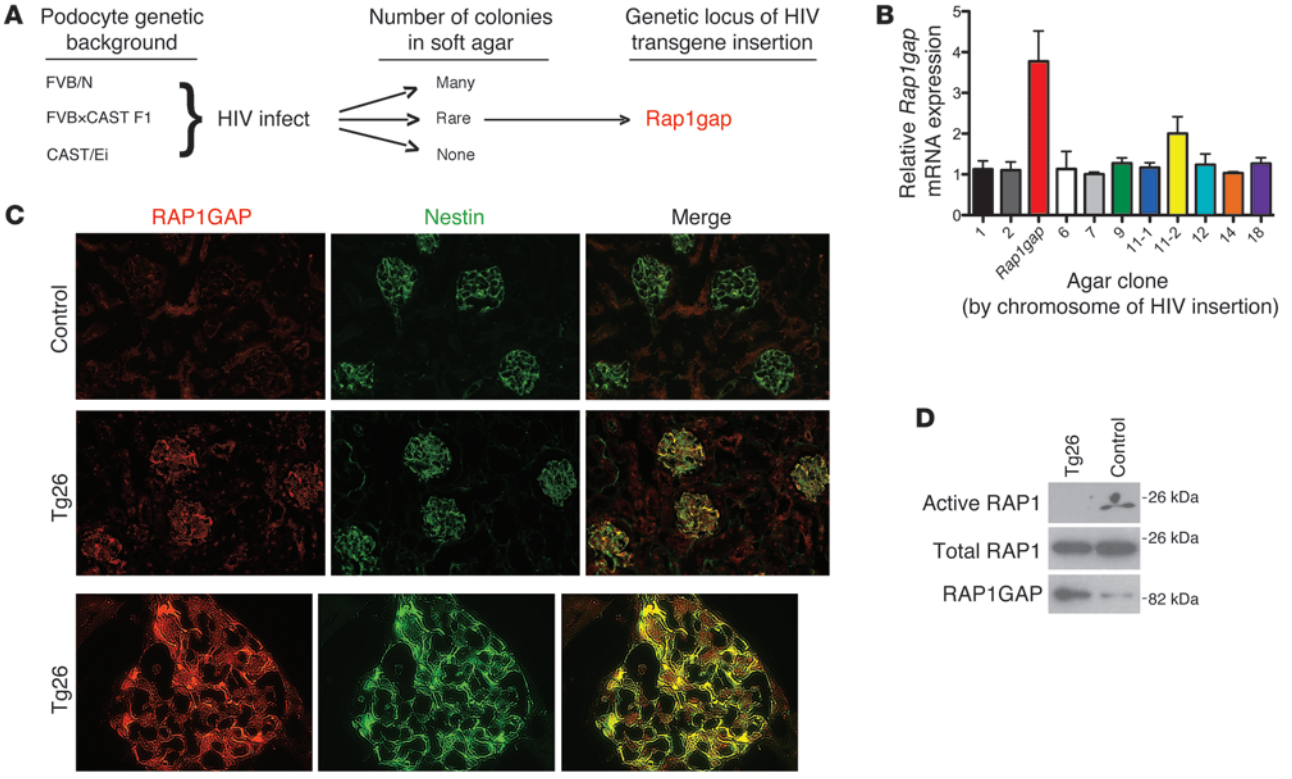

Figure 1
Identification of *Rap1gap* as a candidate gene for mediating podocyte injury after HIV infection. (**A**) Mutagenic screen. Immortalized podocyte cell lines from 3 different genetic backgrounds were generated, infected with HIV-1 provirus, and then grown in soft agar. Podocytes derived from CAST/Ei mice, a background highly resistant to the nephropathy induced by HIV-1 transgene (Tg26) expression, did not show any anchorage-independent growth, whereas cells derived from a highly sensitive background (FVB/N) grew robustly. Podocytes from FVB×CAST F1 mice, while mostly resistant to anchorage-independent growth, did allow for rare colony formation. We hypothesized that these colonies were a direct consequence of HIV-1 proviral integration affecting expression of critical host genes. The HIV-1 integration sites of these clones were mapped, and the candidate gene *Rap1gap* was thus identified. (**B**) The podocyte clone where HIV provirus integrated into the promoter of the *Rap1gap* genetic locus demonstrated markedly higher *Rap1gap* expression compared with podocytes from other clones, as determined by quantitative PCR. (**C**) IF studies demonstrated strongly increased expression of RAP1GAP in podocytes of Tg26 mice compared with controls, as determined by colocalization with the podocyte-specific cytoplasmic protein nestin. Original magnification, ×200 (lower power); ×1,000 (higher power). (**D**) RAP1GAP protein expression was increased in pooled glomerular lysates of Tg26 mice compared with nontransgenic littermates on Western blotting. This was associated with a dramatic loss of glomerular RAP1 activation, as determined by RalGDS-RBD pulldown assays.

in HIV-1 transgenic (Tg26) mice and in human kidney biopsies of focal and segmental glomerulosclerosis (FSGS) and that this resulted in diminished glomerular RAP1 activation. The consequence of loss of podocyte RAP1 signaling was severe both in cell culture and in mice. In fact, mice with podocyte-specific conditional *Rap1a* and *Rap1b* double knockout (referred to herein as DKO mice) developed diffuse severe glomerulosclerosis and died by 2 months. Surprisingly, more mildly haploinsufficient mice also developed severe FSGS, which suggests that smaller changes in RAP1 signaling pathways critically affect podocytes. Furthermore, overexpression of RAP1GAP in cultured podocytes prevented activation of β1 integrin and functionally inhibited β1 integrin–mediated cellular functions. By preventing the RAP1GAP upregulation associated with injury, podocyte cellular adhesion was maintained and detachment prevented, effects that were reversed by specific functional blockade of β1 integrin. Taken together, these results suggest that increased RAP1GAP expression in podocytes, as occurs in human FSGS, contributes directly to podocyte injury by preventing RAP1-mediated activation of β1 integrin.

Results

Identification of Rap1gap as a candidate gene for mediating podocyte injury. Podocyte injury produces a dysregulated phenotype characterized by disruption and reorganization of the actin cytoskeleton, loss of primary processes, and foot process effacement. This is most dramatic in the collapsing variant of FSGS, including HIV-associated nephropathy (HIVAN), in which podocytes lose differentiation markers, proliferate, and show anchorage-independent growth in soft agar (7, 8). In HIVAN in particular, this phenotype is remarkably dependent on the presence of a genetically susceptible host, both in Tg26 mice (9) and in humans (10). We designed and performed a functional genetic screen to identify candidate genes involved in HIV-induced podocyte dysregulation (Figure 1A). To this end, we generated podocyte cell lines from mice of 3 different genetic backgrounds: FVB/Nj, CAST/EiJ, and FVB×CAST F1. Of these, only the FVB background is sensitive to the development of HIV-induced nephropathy (11). When we infected the podocyte lines with HIV-1 virus and then plated each in soft agar, FVB podocytes demonstrated robust anchorage-independent growth form-

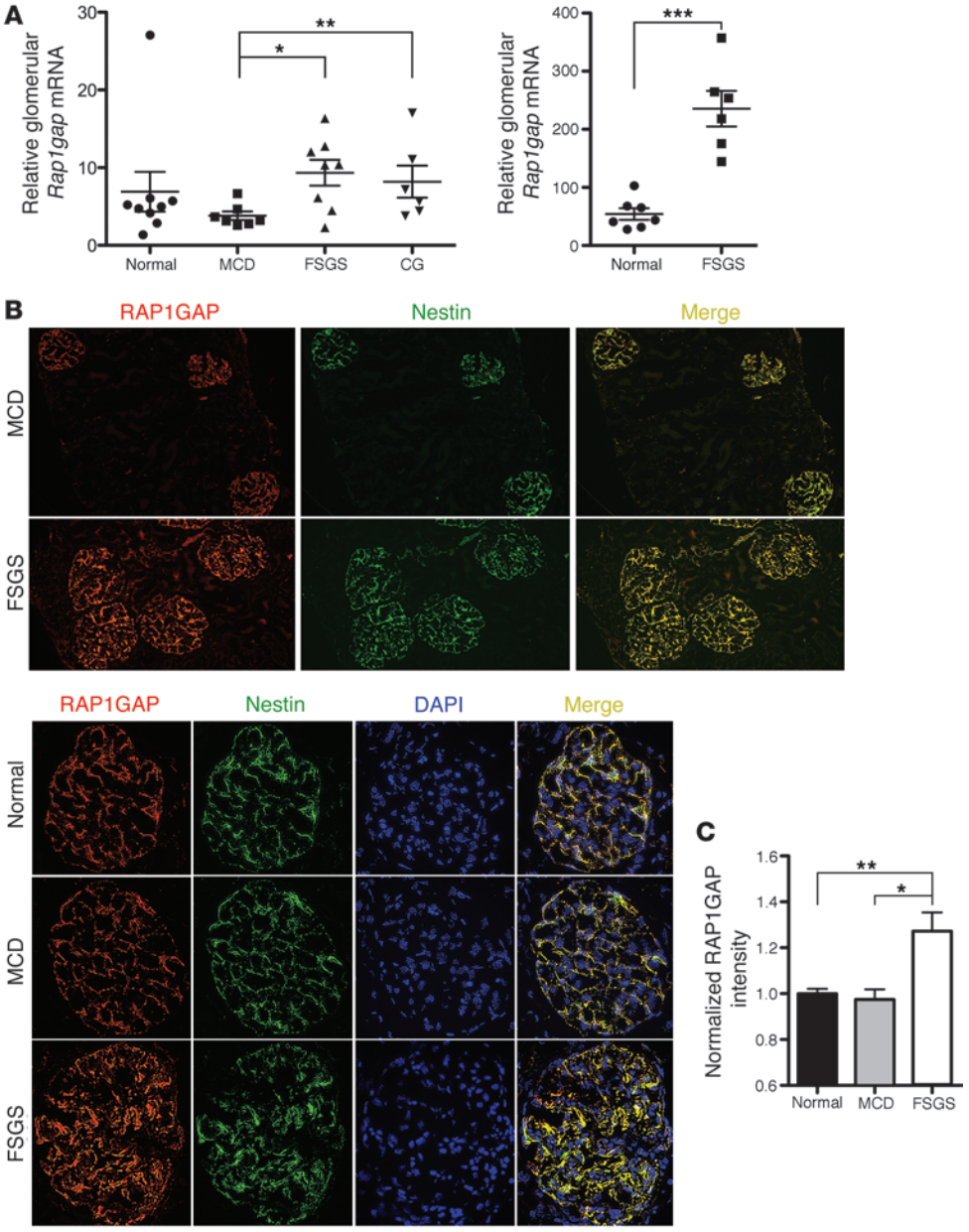

Figure 2

RAP1GAP expression is increased in human FSGS. (**A**) *Rap1gap* mRNA expression was increased in glomeruli of human biopsy specimens with pathological diagnosis of FSGS compared with those with minimal change disease (MCD), collapsing FSGS (CG), or normal. Data are from previously published microarray studies by Hodgin et al. (left; ref. 12) and Bennett et al. (right; ref. 13). The Hodgin et al. data were subjected to further analysis by Nephromine (Compendia Bioscience). $^{*}P < 0.015$, $^{**}P < 0.05$, $^{***}P < 0.0001$. (**B**) IF for RAP1GAP on human kidney biopsy specimens showed robust expression specifically in podocytes in all samples, as determined by colocalization with the podocyte-specific protein nestin. Expression of RAP1GAP was notably stronger, however, in FSGS (n = 5) compared with minimal change disease (n = 5) or normal (n = 4) biopsies. Representative images with identical exposure times are shown. Original magnification, ×100 (lower power); ×400 (higher power). (**C**) Differences in glomerular fluorescent intensity between FSGS and minimal change disease were quantified relative to DAPI using MetaMorph software. All glomeruli from each of the available biopsies were included in the analysis (n = 35 [FSGS], 44 [minimal change disease], 50 [normal]). $^{*}P < 0.005$, $^{**}P < 0.008$.

ing many colonies, whereas CAST cells were completely unable to grow. Interestingly, FVB×CAST F1 podocytes, although genetically resistant, did allow for rare colony formation. We hypothesized that these infrequent events were the direct result of HIV proviral integration affecting the expression of a critical host gene. Using a PCR-based approach, we successfully determined the HIV proviral integration sites for 11 of 18 total FVB×CAST agar clones. One such locus was a region on mouse chromosome 4 near the promoter region of *Rap1gap*. Further testing by quantitative PCR showed that podocytes carrying this insertion had significantly higher expression of *Rap1gap* compared with podocytes from other clones (Figure 1B). This suggested that increased RAP1GAP signaling was sufficient to account for the observed phenotypic change.

Podocytes upregulate RAP1GAP expression levels in FSGS. Expression and function of RAP1GAP in the kidney had not been explored previously. By immunofluorescence (IF), we found a dramatic increase in RAP1GAP expression in podocytes in Tg26 mice compared with nontransgenic littermates (Figure 1C). Double-immunolabeling studies with nestin, a specific marker of podocyte cytoplasm, demonstrated expression of RAP1GAP in podocytes. Increased expression of RAP1GAP protein was confirmed by Western blotting of pooled glomerular lysates of 3 proteinuric Tg26 mice compared with 3 control littermates (Figure 1D). This was accompanied by a marked decrease in glomerular RAP1 activation, as determined by pulldowns using Ral-GDS-RBD agarose.

To corroborate these findings in human glomerular disease, we initially examined data from 2 published microarray studies that compared expression levels of RNA extracted from laser capture–dissected glomeruli from renal biopsy samples (12, 13). Both studies showed significantly increased *Rap1gap* mRNA

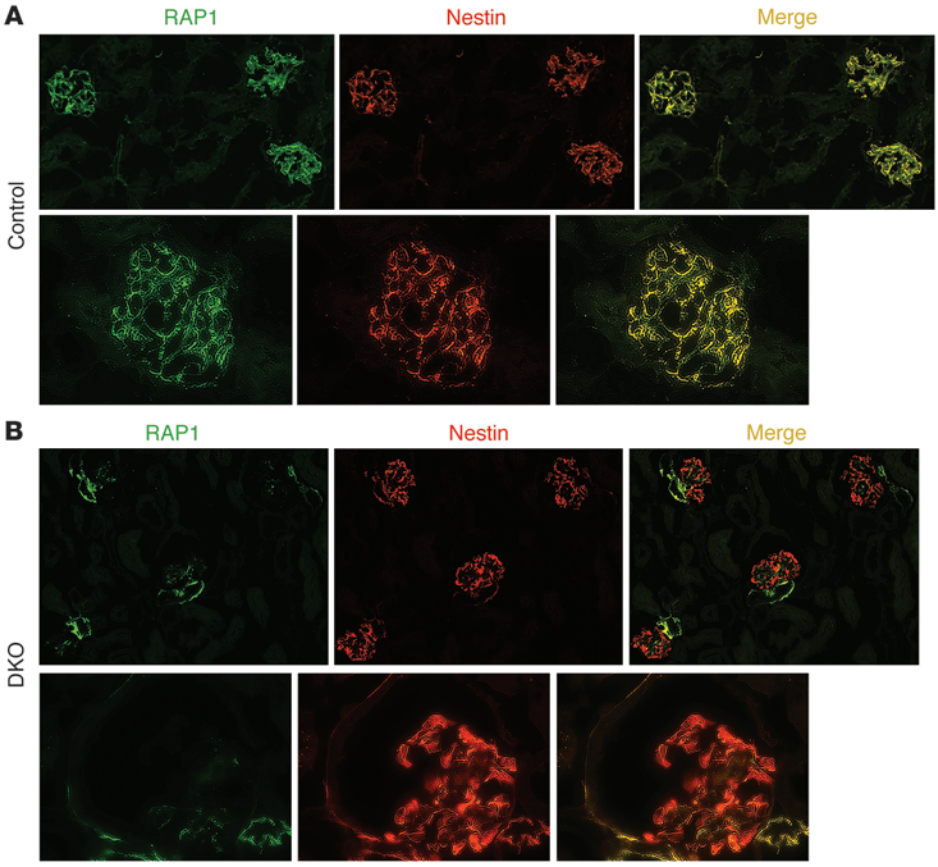

Figure 3
Podocyte expression of RAP1 is lost in DKO mice, floxed *Rap1a*$^{-/-}$ *Rap1b*$^{-/-}$ mice expressing *cre* recombinase under the podocyte-specific podocin promoter. (**A**) Immunostaining for total RAP1 on kidney sections of control mice demonstrated robust expression in podocytes, as determined by colocalization with nestin, a known marker of podocyte cytoplasm. (**B**) In DKO mice, total RAP1 expression in podocytes was lost. Original magnification, ×200 (lower power); ×630 (higher power).

expression in patients with FSGS and/or collapsing FSGS compared with patients with minimal change disease or normal controls (Figure 2A). Interestingly, further analysis of the data from the study by Hodgin et al. (12) using Nephromine (Compendia Bioscience) showed a correlation between glomerular RAP1GAP expression level and disease severity, as determined by percent of glomeruli affected, percent foot process effacement, and degree of renal impairment. To validate these findings, we performed IF analysis of RAP1GAP expression comparing biopsy cases of minimal change disease, FSGS, and normal controls. RAP1GAP was expressed specifically in podocytes in all human samples analyzed, as determined by colocalization with nestin; however, intensity of RAP1GAP staining was clearly strongest in the FSGS samples (Figure 2B). This finding was quantified using MetaMorph software to analyze fluorescent intensity per area, which was normalized to DAPI intensity (Figure 2C). Every glomerulus from each of the available stained biopsies was included in the analysis (n = 35 [FSGS]; 44 [minimal change disease]; 50 [normal]).

Complete podocyte-specific inactivation of both Rap1a and Rap1b in mice induced massive glomerulosclerosis, leading to early death. To begin to examine the in vivo significance of this pathway, we performed IF for RAP1 on normal wild-type murine kidney sections (Figure 3A). Similar to the distribution of RAP1GAP, RAP1 expression was localized primarily in podocyte cytoplasm, as determined by colocalization with the podocyte-specific marker nestin. Such enhanced expression of RAP1 and RAP1GAP in podocytes suggests that these molecules may have a particularly important role in these cells.

Because *Rap1a* and *Rap1b* double-knockout mice are early embryonic lethal (14, 15), in vivo studies of their roles in podocytes required the use of conditional knockouts. To accomplish this, floxed *Rap1a* (16) and floxed *Rap1b* conditional knockout mice (16) were bred to transgenic mice expressing *cre* recombinase under the podocyte-specific podocin promoter. We were thus able to generate podocyte-specific *Rap1a*$^{-/-}$, *Rap1b*$^{-/-}$, and combined DKO mice. IF studies directed at total RAP1 confirmed the absence of glomerular RAP1 expression in DKO mice (Figure 3B). Most DKO animals died from renal failure and massive proteinuria by 8 weeks of age (Figure 4, A and B). Pathological analysis at 3 weeks revealed severe and diffuse mesangial expansion and sclerosis as well as overlying swollen and hypertrophied podocytes (Figure 4C). This process progressed rapidly with age and affected all glomeruli. At 3 weeks of age, some glomeruli showed early collapse with overlying epithelial cell proliferation. Diffuse mesangial expansion has been described in other mouse models of severe podocyte injury, in particular those that induce major podocyte depletion, including CD2AP-null (17) and podocin-null (18) mice. By 6 weeks of age, mice demonstrated massive segmental and global glomerulosclerosis involving all glomeruli (Figure 4D). A prominent pathological feature was glomerular collapse with extensive epithelial cell hyperplasia and proliferation with pseudocrescents as well as large tubular microcysts, pathological features reminiscent of severe HIVAN. The presence of mitotic figures and high glomerular Ki-67 expression levels (Figure 4E) were consistent with this proliferative phenotype. Besides epithelial proliferation, podocytes also displayed a high rate of apoptosis, as visualized by nuclear fragmentation and chromatin condensation.

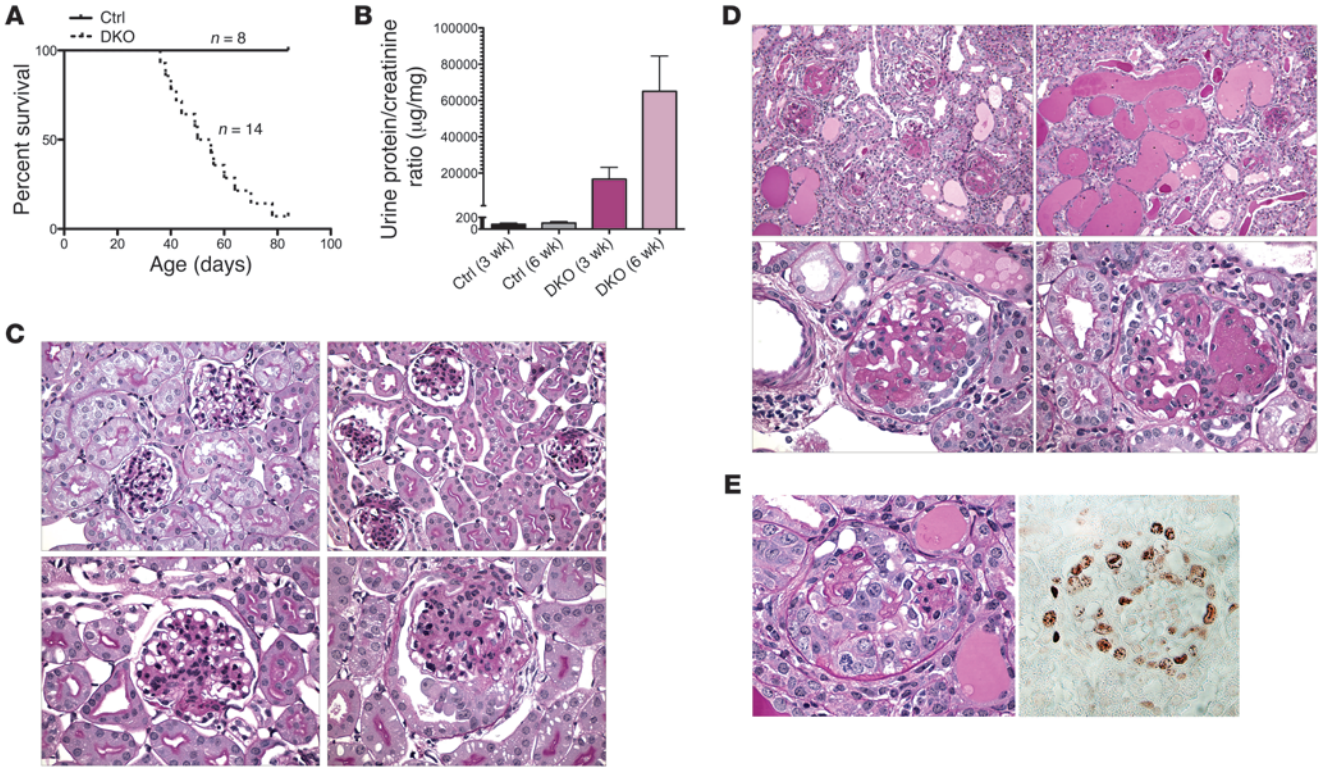

Figure 4

Podocyte-specific inactivation of both *Rap1a* and *Rap1b* induces massive glomerulosclerosis and death. (**A**) The majority of DKO mice died by 8 weeks of age. (**B**) Calculated urine protein/creatinine ratios confirmed massive proteinuria in DKO versus control mice. (**C**) Kidney histology from mice aged 3 weeks. Control mice demonstrated patent glomerular capillaries with a normal-appearing mesangium (top left). DKO mice (top right and bottom row) showed severe mesangial expansion affecting all glomeruli. Some glomeruli demonstrated early lesions of segmental sclerosis with overlying epithelial hyperplasia (bottom left). (**D**) By 6 weeks of age, DKO renal pathology drastically worsened. There was diffuse and severe glomerulosclerosis affecting all glomeruli, giving the kidney an end-stage appearance (top left). The interstitium showed widespread tubular microcysts with diffuse proteinaceous casts (top right). A prominent feature was collapsing glomerulosclerosis with overlying epithelial cell hypertrophy and hyperplasia (bottom row). (**E**) Glomerular collapse was often severe, with prominent pseudocrescent formation. Immunostaining of a serial section confirmed strong glomerular Ki-67 expression. Original magnification, ×400 (**C**, top); ×200 (**D**, top); ×600 (**C** and **D**, bottom, and **E**).

Podocytes could be seen detaching from the GBM leading to large foci of denudation.

Electron microscopic analysis reinforced many aspects of the phenotype (Figure 5A). At 3 weeks of age, glomerular capillary loops remained patent, but podocytes showed diffuse and complete foot process effacement with severe microvillous transformation of their cytoplasm. There was severe loss of primary and secondary process formation. In some cases, the cell bodies seemed to sit directly on the GBM without any intervening process maturation whatsoever. The mesangial matrix was increased. Later, by 6 weeks of age, the entire glomerulus had been replaced by ECM, with surrounding remnant epithelial cells occupying Bowman's space. Open capillary loops were rare and, when present, showed complete podocyte effacement characterized by unusual broad intercellular contacts resembling desmosomes. Extensive podocyte cytoplasmic vacuolization was evident, as well as broad areas of podocyte detachment causing GBM denudation (Figure 5B). Many glomerular capillaries were narrowed or occluded by ECM, with overlying effaced podocytes that displayed pale cytoplasm and irregularly shaped secondary processes and cell bodies.

Partial Rap1 haploinsufficiency also induces severe FSGS. Surprisingly, even partial podocyte-specific *Rap1* haploinsufficiency was sufficient to induce severe glomerular injury. Mice that carried a single intact *Rap1* allele (i.e., loss of 3 of 4 *Rap1* alleles) in podocytes still developed severe FSGS, although comparatively more moderate than that in DKO mice. This phenotype was the same whether the intact allele was *Rap1a* or *Rap1b*. Many of these mice died by 4 months of age due to the effects of heavy proteinuria (Figure 6, A and B), despite intact kidney function. We observed moderate mesangial expansion affecting all glomeruli, accompanied by variable amounts of FSGS involving 5%–40% of glomeruli (Figure 6C). Here, segmental sclerosis and mesangial expansion coexisted, and both worsened over time. The tubular microcystic disease observed in complete haploinsufficiency was absent. Onset of dipstick-positive proteinuria was sudden, usually beginning at 4–7 weeks of age. All animals that developed proteinuria died early. Approximately 40% of animals of this genotype did not become proteinuric and did not die early. The reason for this is uncertain, but may reflect differences in genetic background. Electron microscopy revealed diffuse foot process effacement with microvillous transformation (Figure 6D). Podocyte cell shape was severely abnormal, with a pale and vacuolated cytoplasm that often lacked normal primary and secondary process architecture. The GBM often appeared wrinkled, consistent with a collapsing phenotype. Podocyte detachment was again evident.

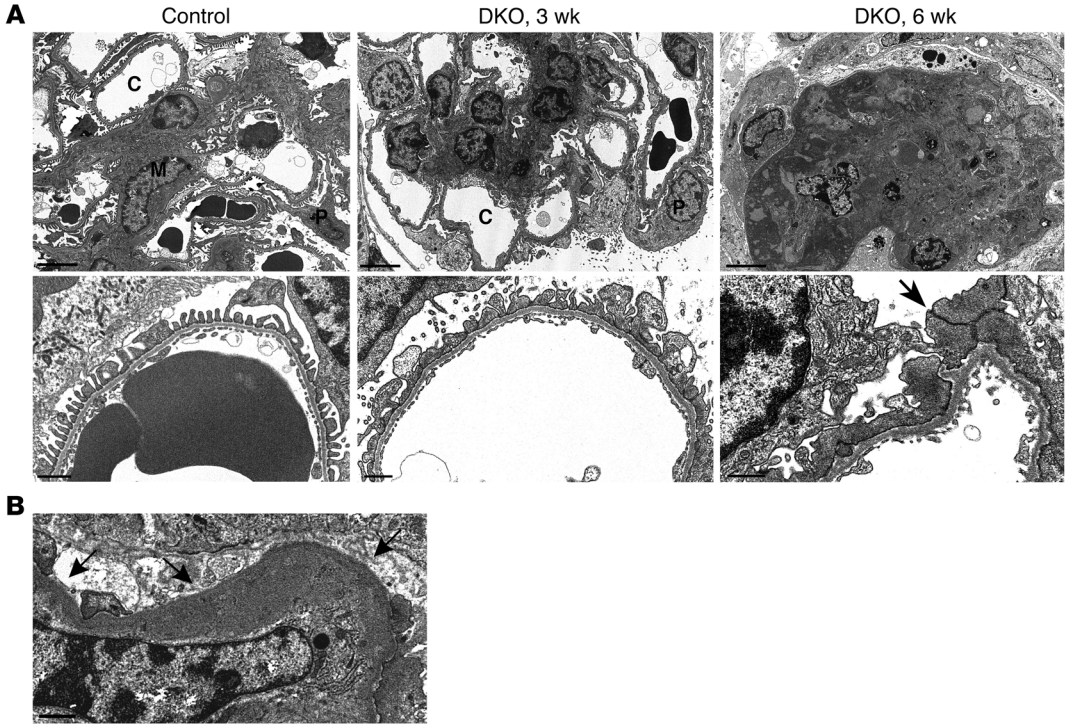

Figure 5
Electron micrographic studies of DKO mice, showing time course and extent of podocyte dysfunction. (**A**) Control kidney exhibited open capillary loops, delicate foot processes, and a normal-appearing mesangium (M). By 3 weeks of age, DKO kidneys showed severe podocyte injury accompanied by dramatic mesangial expansion. Foot processes were completely effaced, and podocyte (P) cell bodies had a simplified cellular shape with few primary or secondary processes and severe microvillous transformation. At 6 weeks, most DKO glomeruli were replaced by severe sclerosis completely obliterating the majority of capillary lumens (C). Remnant glomerular epithelial cells filled the remainder of Bowman's space. Remaining rare open capillary loops showed complete podocyte effacement with unusual desmosomal-like intercellular contacts (arrow). Scale bars: 5 μm (top); 2 μm (bottom). (**B**) DKO glomeruli showed severe podocyte detachment with areas of denuded glomerular basement membrane (arrows). Scale bar: 1 μm.

Glomerular collapse with epithelial cell proliferation is a major pathological feature, which includes robust Ki-67 expression. Consistent with this component, we observed a dramatic loss of expression of the podocyte differentiation marker synaptopodin in all glomeruli, although not as total as that in DKO mice (Figure 6E). This phenotype was again reminiscent of the collapsing glomerulopathy characteristic of HIVAN.

Podocyte detachment, including areas of denuded GBM, is also prominent. Such podocyte loss is known to be a major driving force of FSGS pathogenesis. To investigate podocyte number in *Rap1*-deficient mice, we calculated the average number of podocytes per glomerular area by counting WT1-positive podocytes (Figure 6F). For DKO mice, there was dramatic and progressive loss of WT1 expression. By 6 weeks of age, in fact, WT1 expression was mainly lost, probably a reflection of both severe podocyte loss and diffuse glomerulosclerosis. *Rap1*-haploinsufficient mice also showed significant loss of podocytes, although less severe than that in DKO mice.

Increased RAP1GAP expression in podocytes causes loss of activated β1 integrin. To investigate the mechanism by which increased podocyte expression of RAP1GAP leads to injury, we used a lentiviral-based vector to deliver and overexpress RAP1GAP in cultured human podocytes. These cells expressed dramatically higher levels of RAP1GAP and lower amounts of GTP-bound RAP1 at baseline compared with control podocytes transduced with vector alone (Figure 7A). In other cell types, RAP1-GTP has been shown to be an important mediator of inside-out integrin activation (19, 20). In podocytes, α3β1, the predominant integrin expressed, is indispensable for proper function; in fact, in mice, podocyte-specific deletion of β1 integrin results in severe proteinuria with early lethality (21, 22). We therefore hypothesized that RAP1GAP upregulation directly contributes to podocyte dysfunction by preventing RAP1-GTP–mediated activation of β1 integrin. To examine this possibility, we analyzed the levels of active β1 integrin on the cell surface by flow cytometry. Podocytes overexpressing RAP1GAP showed dramatically reduced staining of 12G10, a monoclonal antibody that specifically recognizes the activated conformation of β1 integrin, compared with control cells (Figure 7B). β3 integrin is the other β integrin expressed by podocytes. To test the effects of RAP1GAP overexpression on activation of β3 integrin, we performed FACS analysis using monoclonal antibody AP5, which specifically recognizes its activated conformation. At baseline, there was no difference in levels of activated β3 integrin comparing RAP1GAP-overexpressing and control podocytes (Figure 7B). Furthermore, basal levels of activated β3 integrin (AP5 binding) were dramatically lower than for β1 integrin (12G10 binding). Importantly, RAP1GAP overexpression did not alter levels of total β1 integrin or total β3 integrin, as determined by Western blot-

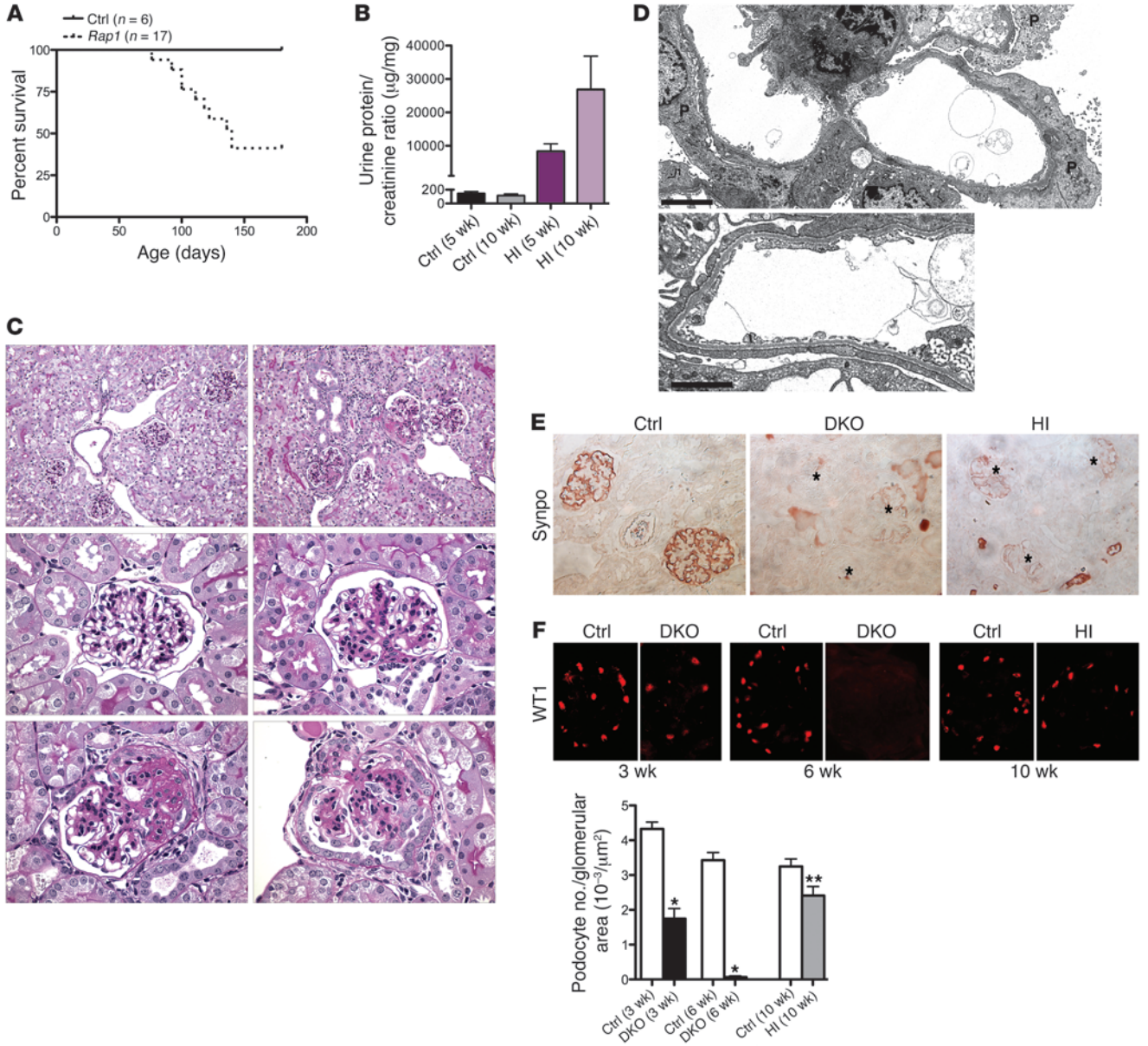

Figure 6

Podocyte-specific *Rap1* haploinsufficiency induces FSGS. (**A**) Mice with 1 functional copy of *Rap1* developed proteinuria and early death. All animals that developed proteinuria (60% overall) died early. HI, haploinsufficient. (**B**) Calculated urinary albumin/creatinine ratios showed heavy proteinuria. (**C**) Representative pathology for 6-week-old *Rap1*-haploinsufficient mice. Top: Whereas age-matched controls (left) exhibited normal histology, in haploinsufficient mice (right), 2 of 3 glomeruli showed severe segmental lesions. Middle: Control glomeruli (left) showed delicate mesangium, compared with moderate mesangial expansion affecting most glomeruli in haploinsufficient mice (right). Bottom: Many of these lesions progressed to FSGS (left), in which collapsing glomerulopathy was a prominent feature (right). (**D**) On electron microscopy, podocytes demonstrated complete foot process effacement with microvillous transformation and loss of normal primary and secondary process architecture. Scale bars: 5 μm (top), 2 μm (bottom). (**E**) Synaptopodin expression was completely lost in DKO mice and severely diminished in haploinsufficient mice, even in nonsclerotic glomeruli. (**F**) Severe podocyte loss was evident in DKO mice. Podocyte loss was present, but to a lesser extent, in haploinsufficient mice. A representative WT1-stained glomerulus for each group is shown. The number of WT1-positive cells per glomerular tuft area was determined for approximately 20–30 glomeruli per animal. n = 2–4 mice per group. $^*P < 0.001$, $^{**}P < 0.02$ versus age-matched WT control. Original magnification, ×200 (**C**, top); ×600 (**C**, middle and bottom); ×400 (**E**); ×630 (**F**).

ting (Figure 7A). These results suggest that podocyte RAP1GAP upregulation functionally inhibits activation of β1, but not of β3.

To investigate the effects of increased podocyte RAP1GAP expression on β1 integrin–mediated cellular functions, we analyzed cells with respect to adhesive strength, migration, and induction of intracellular signaling. Podocytes overexpressing RAP1GAP adhered significantly less strongly to fibronectin and laminin than did control cells (Figure 7C). Furthermore, RAP1GAP overexpres-

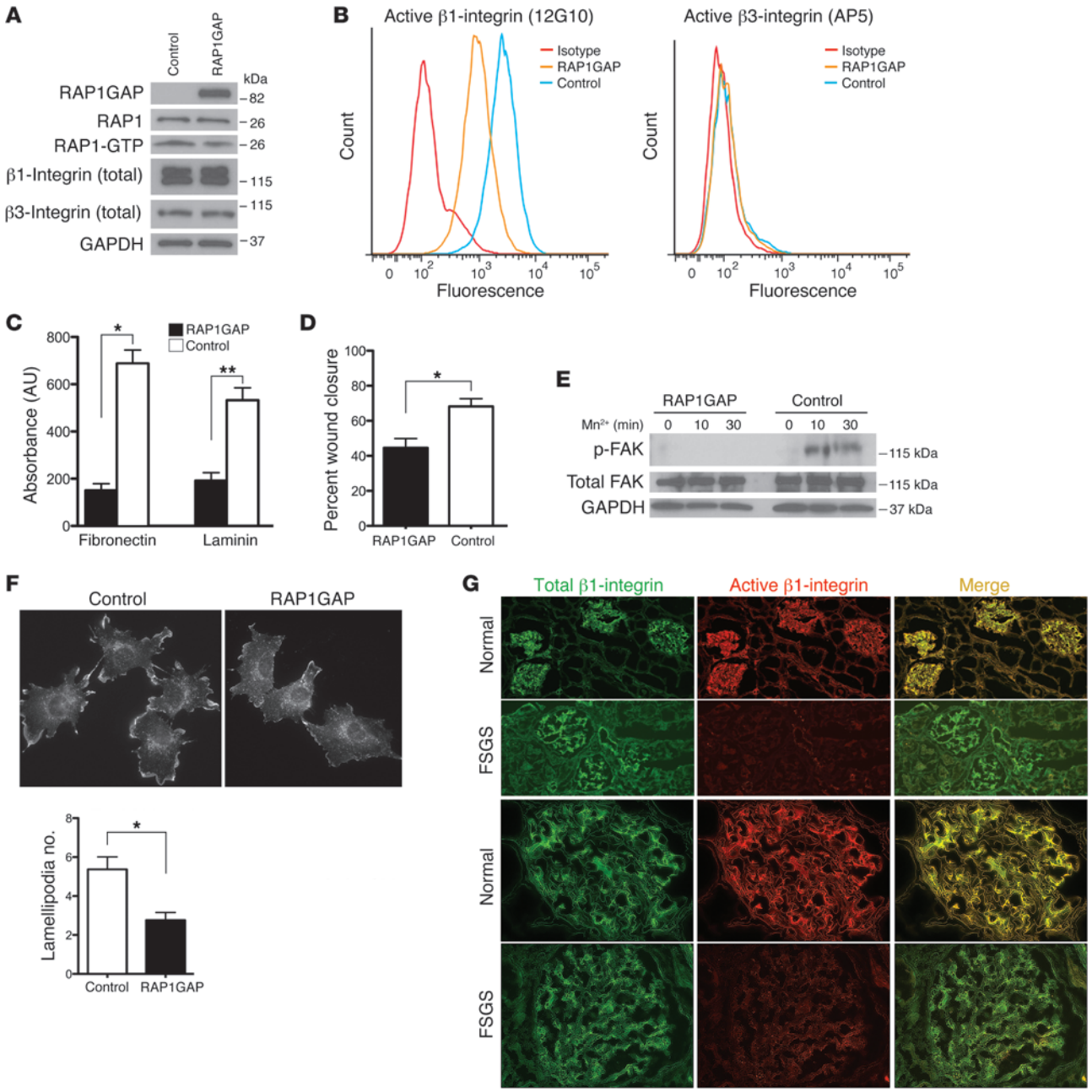

Figure 7

RAP1GAP overexpression in podocytes results in diminished activation of β1 integrin. (**A**) Podocytes transduced with a RAP1GAP expression plasmid showed higher RAP1GAP protein levels compared with cells transduced with vector alone, but expression of total β1 and β3 integrin was identical between the 2 groups. (**B**) FACS analysis of podocytes transduced as indicated was performed using antibodies 12G10 and AP5, which specifically recognize the active conformation of β1 integrin and β3 integrin, respectively. RAP1GAP podocytes showed dramatically reduced binding of 12G10, but binding of AP5 was unchanged. Representative histograms are shown. (**C**) Cellular adhesion to GBM components was diminished in RAP1GAP cells. Calorimetric quantitation is shown. Data represent the mean of 2 independent experiments performed in triplicate. *$P < 0.002$, **$P < 0.004$. (**D**) RAP1GAP podocytes migrated and closed a scratch made in a confluent monolayer more slowly than control cells. Quantification shows the average percent wound closure at predetermined locations along the scratch. *$P < 0.003$. (**E**) Transduced podocytes were exposed to 1 mM Mn^{2+}, a potent integrin activator, for a set amount of time prior to harvesting protein lysates for Western blotting. RAP1GAP podocytes were resistant to integrin-mediated FAK phosphorylation. (**F**) RAP1GAP podocytes had fewer lamellipodia, as determined by cortactin staining. Quantitation of lamellipodia number was performed on randomly selected differentiated podocytes ($n = 100$ per group, repeated 3 times). *$P < 0.001$. (**G**) Human kidney biopsy sections were simultaneously stained for total (antibody EP1041Y) and activated (antibody 12G10) β1 integrin. Glomeruli from biopsies of FSGS showed a greater loss of activated relative to total β1 integrin. Original magnification, ×630 (**F**); ×100 (**G**, lower power); ×400 (**G**, higher power).

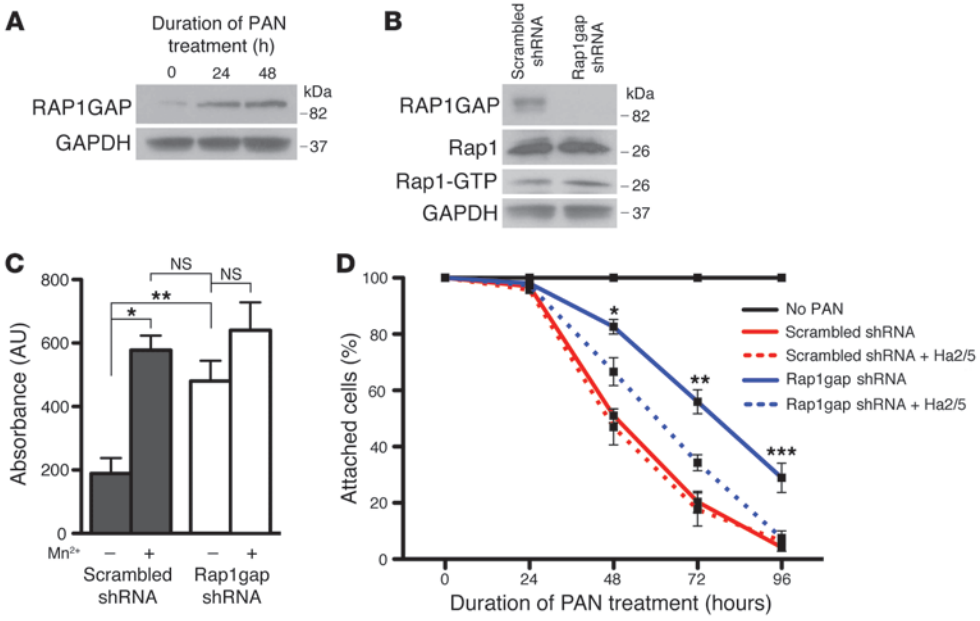

Figure 8

RAP1GAP silencing prevents podocyte detachment after injury by preserving β1 integrin–mediated adhesion. (**A**) Podocyte injury by exposure to PAN induced increased RAP1GAP protein expression. (**B**) A podocyte cell line that expresses an shRNA targeting *Rap1gap* expressed lower amounts of RAP1GAP protein and showed increased basal activation of RAP1 compared with podocytes carrying a scrambled shRNA. (**C**) RAP1GAP silencing dramatically increased podocyte adhesion to fibronectin. The increase in adhesive strength caused by loss of RAP1GAP was similar to that caused by the potent integrin activator Mn^{2+}. $^{*}P < 0.0005$, $^{**}P < 0.007$. (**D**) RAP1GAP-silenced podocytes were protected from PAN-induced cellular detachment. This protection was lost, however, when cells were treated with the β1 integrin–blocking antibody Ha2/5. $^{*}P < 0.0001$, $^{**}P < 0.0001$, $^{***}P < 0.0001$, ANOVA. See Results for individual *t* tests.

sion induced an inability to migrate effectively, as measured by how quickly podocytes were able to close a wound inflicted on a confluent monolayer (Figure 7D). Ligand binding also initiates a complex intracellular signaling cascade through recruitment and activation of nonreceptor tyrosine kinases, including focal adhesion kinase (FAK) (23). Divalent cations, in particular Mn^{2+}, induce direct activation of integrins through a mechanism that requires RAP1-GTP (24). Podocytes overexpressing RAP1GAP were resistant to integrin-mediated FAK phosphorylation by Mn^{2+} (Figure 7E), consistent with a diminished ability for integrin activation in these cells. Proper integrin activation is also essential for normal lamellipodia formation (25). RAP1GAP podocytes demonstrated fewer and less prominent lamellipodia, as determined by staining for cortactin, a marker of formed lamellipodia (Figure 7F). Control podocytes showed robust recruitment of cortactin to lamellipodia, whereas in RAP1GAP podocytes, cortactin remained more cytoplasmic. Overall, these assays demonstrated that increased RAP1GAP expression in podocytes functionally inhibited β1 integrin, consistent with its ability to prevent RAP1-GTP–mediated integrin activation.

We next sought to determine whether increased podocyte expression of RAP1GAP correlates with diminished podocyte activation of β1 integrin in human kidney disease. Although there has been some suggestion that total glomerular β1 integrin expression decreases modestly in human FSGS (26), relative amounts of activated β1 integrin have not been studied. To investigate this, we did double IF for both total (antibody EP1041Y) and activated (antibody 12G10) β1 integrin on human kidney biopsy samples (Figure 7G). In normal human kidney and in minimal change disease, there was robust expression of both total and activated β1 integrin. However, in several FSGS biopsies, there was a dramatic loss of podocyte glomerular expression of activated β1 integrin relative to total β1 integrin. This finding implicates RAP1GAP upregulation in podocytes as a potential mechanism for loss of glomerular β1 integrin activation in human FSGS.

Loss of RAP1GAP expression maintains β1 integrin–mediated adhesion in injured podocytes. Having established that upregulated RAP1GAP was harmful to podocyte function, we next asked whether preventing this increase after injury might preserve β1 integrin activity and cellular function. We used the puromycin aminonucleoside (PAN) model of podocyte injury, because RAP1GAP expression levels were increased in PAN-treated cultured murine podocytes (Figure 8A) and because cellular detachment is a prominent part of the PAN-induced phenotype. To prevent RAP1GAP upregulation, we introduced an shRNA that targets *Rap1gap* into a conditionally immortalized mouse podocyte line using a lentiviral delivery system. Podocytes carrying this shRNA expressed dramatically lower levels of RAP1GAP by Western blotting compared with control cells infected with a scrambled shRNA (Figure 8B). This was associated with increased basal expression of RAP1-GTP in the RAP1GAP knockdown podocytes. Attempts to directly analyze differences in cell surface activation of β1 integrin by flow cytometry were unsuccessful, presumptively because 9EG7, the only commercially available anti-mouse antibody specific for an activated β1 epitope, fails to bind to activated β1 when it is associated with α3 (27). However, these cells clearly had increased β1 integrin function, as determined by dramatically increased cellular adhesion to fibronectin (Figure 8C). In fact, RAP1GAP knockdown cells were as strongly adhesive as podocytes that had been treated with Mn^{2+}, a stimulus that leads to maximal integrin activation. To examine the effects of RAP1GAP suppression on podocyte injury, we exposed podocytes to PAN and examined its effect on cellular detachment and apoptosis (Figure 8D and Supplemental Figure 1; available online with this article; doi:10.1172/JCI67846DS1). RAP1GAP silencing dramatically protected podocytes from detachment compared with control cells (48 hours, $P < 0.0005$; 72 hours, $P < 0.0004$; 96 hours, $P < 0.002$) and also markedly protected against apoptosis. Treating podocytes with the β1 integrin functional blocking antibody Ha2/5 reversed this effect and caused RAP1GAP-silenced podocytes to detach (48 hours, $P < 0.03$; 72 hours, $P < 0.006$; 96 hours, $P < 0.004$). In fact, by 96 hours after addition of PAN,

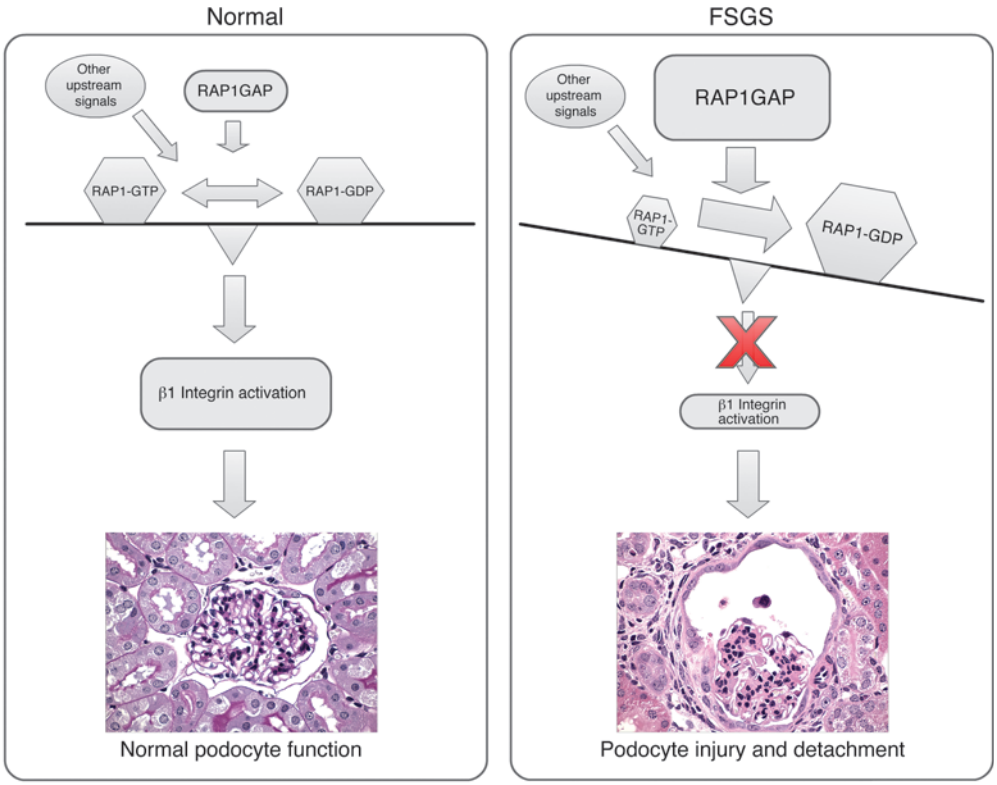

Figure 9
Increased podocyte expression of RAP1GAP drives podocyte injury by preventing activation of β1 integrin. In normal podocytes, several upstream signals, including RAP1GAP, converge to maintain proper cellular RAP1 homeostasis and appropriate β1 integrin–mediated adhesion and signaling. In FSGS, however, increased podocyte expression of RAP1GAP leads to inhibition of RAP1-GTPase and relative accumulation of RAP1 as RAP1-GDP. This leads to a reduction in activated β1 integrin, including reduced adhesion to GBM components. We propose that this pathway is an important mediator of podocyte detachment from the GBM, a process characteristic of podocyte loss in human glomerular diseases such as FSGS. Images shown are from a control and a podocyte-specific *Rap1*-haploinsufficient mouse (original magnification, ×600).

RAP1GAP-silenced podocytes treated with Ha2/5 were almost completely detached, similar to control podocytes, whereas RAP1GAP-silenced podocytes not subjected to β1 integrin blockade were still almost 30% attached. ANOVA values were highly significant at the 48-, 72-, and 96-hour time points ($P < 0.0001$). These results suggest that silencing RAP1GAP in podocytes may protect them from injury by preserving β1 integrin–mediated cellular functions.

Discussion

In the current work, we used a functional genomic approach to identify genes that, when dysregulated, are critical to mediating podocyte injury. To accomplish this, we designed a novel insertional mutagenic screen whose readout was the ability of genetically resistant podocytes to clonally proliferate in soft agar after HIV infection. Several aspects of the screen were innovative. First, we used HIV-1 provirus both as a source of podocyte injury and as an insertional mutagenic element. Previous studies have shown that HIV-1 integration can occur not only in exons and introns of transcriptionally active genes, but also into noncoding sequences near transcription start sites (28–30). The consequences of this integration can therefore result in altered host gene product, or it can cause increased or decreased expression levels of host genes (31–33). Second, for the screen to be successful, we needed to select an appropriate genetically resistant podocyte cell line in which the consequences of HIV-1 proviral integration might induce susceptibility. We hypothesized that heterozygous podocytes, carrying 1 susceptible and 1 resistant allele (FVB×CAST F1), would be more vulnerable to mutagenesis than a homozygous resistant line (CAST). Indeed, whereas pure CAST podocytes were completely resistant to anchorage-independent growth, FVB×CAST F1 cells gave rare colony formation after HIV infection. Third, because our screen selected mutated genes based on their ability to induce a functional change, we hypothesized that identified candidates had a high likelihood of being biologically relevant. This differs dramatically from methods such as RNA-seq, which generates a long list of dysregulated genes without any functional correlation.

In this way, we identified 11 genetic loci based on the HIV-1 proviral integration sites of their agar clones. We selected *Rap1gap* for further studies for several reasons. *Rap1gap* had never previously been described in podocytes, but existing functional studies in other cell types suggested its potential importance as a modulator of cytoskeletal dynamics. We were also intrigued that proviral integration had occurred near the promoter region of this gene on chromosome 4, implying that integration may have affected gene expression. Indeed, quantitative PCR showed that the podocyte colony carrying this insertion had significantly higher expression of RAP1GAP compared with podocytes from other clones. This suggested that increased expression of RAP1GAP may account for the observed functional change and validated the need for further studies.

We next demonstrated that RAP1GAP expression was dramatically increased in injured podocytes in FSGS, both in mouse models and on human kidney biopsy specimens. The cause of increased RAP1GAP expression in this disease is unclear. Recently, mapping studies of the *Rap1gap* promoter revealed several putative bHLH transcription factor binding sites that strongly drove protein expression in RAP1GAP promoter/luciferase reporter assays (34). In FSGS, it is unknown whether expression of these transcription factors is involved in RAP1GAP upregulation. We believe that FSGS is the first human disease known to be associated with elevated RAP1GAP levels; on the contrary, several human diseases, mainly malignancies, are strongly associated with RAP1GAP downregulation. The mechanism of this is mediated by promoter

methylation (5, 6), proteasomal degradation (35), and loss of heterozygosity (36). It is unclear whether these factors also play a role in driving RAP1GAP expression in injured podocytes in FSGS.

We showed that the effect of RAP1GAP upregulation in podocytes — decreased signaling through RAP1-GTP — had a major role in inducing podocyte dysfunction. Interestingly, others have reported that global knockout of either *Rap1a* or *Rap1b* has only subtle phenotypes, without any described renal defects (14, 37, 38). Global *Rap1a*$^{-/-}$ *Rap1b*$^{-/-}$ double-knockout mice are early embryonic lethal (14, 15), making it impossible to assess the effects of complete *Rap1* haploinsufficiency in adulthood. This finding also suggests some functional redundancy between these RAP1 isoforms, which differ by only 9 amino acids, share 95% identical amino acid sequences, and are highly conserved in all mammals. To investigate the effects of complete loss of *Rap1* specifically in podocytes, we generated DKO mice with podocyte-specific combined *Rap1a* and haploinsufficiency. Podocytes from DKO animals seemed to develop normally based on light and electron microscopic analysis of mice on the first day of birth (data not shown); however, they rapidly became injured, leading to mesangial expansion, massive glomerulosclerosis affecting all glomeruli, and death. Interestingly, haploinsufficient mice with only 1 intact allele of either *Rap1a* or *Rap1b* also developed FSGS. The kidney disease in these mice, while less dramatic than that of full DKO mice, was still severe, including moderate mesangial expansion in all glomeruli and severe FSGS. Because the kidney phenotype is identical whether the intact allele was *Rap1a* or *Rap1b*, these 2 isoforms in podocytes seem to be largely functionally redundant.

In FSGS, podocyte loss, including detachment from the GBM, is a major contributor to disease pathogenesis, but the mechanisms driving this process are not well understood. In the current work, we describe a novel mechanism that may be a critical mediator of this process (Figure 9). In normal podocytes, RAP1GAP is in balance with other upstream signals that maintain appropriate cellular levels of RAP1-GTP that can then adequately activate β1 integrin. In podocytes in FSGS, upregulated RAP1GAP leads to overall diminished cellular RAP1-GTP and therefore less activated β1 integrin. We propose that this loss of activated β1 integrin may be a critical mediator of podocyte loss and detachment from the GBM in FSGS. Because RAP1 sits at the center of a large signaling network with effects on many major biological processes (2), we cannot rule out that other RAP1 signaling pathways may also play a significant role in podocyte function.

An important ongoing question is whether preserving RAP1 signaling in podocytes could help to protect them from injury. Our cell culture data suggest that this may be true, by a mechanism involving preservation of activated β1 integrin. Future studies in mice will be needed to confirm this finding and to better explore therapeutic possibilities. What is clear, however, is that podocytes were highly sensitive to changes in RAP1 signaling and that tight regulation of this pathway was required to maintain normal glomerular homeostasis. Diminished RAP1-GTP, as mediated by elevated RAP1GAP levels, is likely an important factor in inducing podocyte dysfunction in human glomerular diseases such as FSGS.

Methods

Mutagenic screen. Immortalized podocyte cell lines were generated as follows. Isolated glomeruli were grown on type I collagen–coated dishes in RPMI 1640 containing 10% FBS supplemented with 1% insulin/transferring/selenium A and 100 U/ml penicillin. After 5 days of growth, cellular outgrowths were detached with trypsin and passed through a 25-μm sieve. These cells were then replated, and the following day were infected with a VSV-pseudotyped retrovirus expressing the TsSV40 large tumor antigen containing the G418 resistance gene. Cells were subsequently plated at 33°C in medium containing G418 (400 μg/ml) and IFN-γ (100 U/ml) and allowed to grow for at least 1 month. Clonal cell populations were then grown using NIH 3T3 as feeder cells as described previously (39). Individual podocyte cellular clones were thermoshifted to 37°C without IFN-γ for 10 days, and those with high expression of WT1 and synaptopodin by immunohistochemistry were selected for further studies.

Podocytes were infected with VSV-pseudotyped gag/pol–deleted HIV-1 provirus (pNL4-3: ΔG/P-EGFP) and then grown in soft agar as previously described (8). After 4 weeks of growth, individual colonies were harvested, and each was divided for genomic DNA and total RNA extraction. Identification of host HIV integration site was done using an established protocol (40). Briefly, genomic DNA was digested with the restriction enzyme MseI. A compatible linker DNA sequence was then ligated to the digested DNA. To prevent PCR amplification of the 5′ LTR, products were then digested with SacI. 2 rounds of nested PCR were performed with forward primers on the 3′ LTR and the reverse primers derived from the linker adaptor. After gel purification, host genomic DNA was sequenced using a primer sequence derived from the linker that was inside of the nested PCR. Identified DNA sequences were then analyzed using NCBI BLAST to determine exact host HIV integration site.

Antibodies. The following antibodies were used: RAP1 (Millipore, 17-321, Western blotting), RAP1 (BD Biosciences, 610195, IF), RAP1GAP (Epitomics, 1530-1, Western blotting and IF), activated β1 integrin (Millipore, clone 12G10), total β1 integrin (BD Biosciences, clone 18), total β1 integrin (Millipore, clone EP1041Y), β1 integrin functional blocking (BD Biosciences, Ha2/5), total β3 integrin (Cell Signaling, D7X3P), activated β3 integrin (AP5, BloodCenter of Wisconsin), cortactin (Millipore, clone 80/85), total FAK (Cell Signaling, catalog no. 3285), Phospho-FAK (Cell Signaling, Tyr576/577, catalog no. 3281), WT1 (Santa Cruz Biotechnology, C-19), synaptopodin (G1, courtesy of P. Mundel, Harvard University, Boston, Massachusetts, USA), Ki-67 (BD Biosciences, 550609), nestin (BD Biosciences, 556309, mouse IF), nestin (Santa Cruz Biotechnology, 10C2, human IF).

Digital image analysis. Images of all glomeruli of immunostained human kidney biopsies were taken at ×40, ×63, or ×100 magnification at the Icahn School of Medicine at Mount Sinai Microscopy Shared Resource Facility. A fixed exposure time was set based on the fluorescence intensity of the most strongly fluorescent glomeruli. To determine intensity of staining, we drew a region of interest around each glomerulus and then measured the mean luminosity of the region using the software analysis program MetaMorph. A similar approach was used to determine the mean luminosity of DAPI.

Mice. Podocin *cre* transgenic mice were previously described (41) and genotyped by the same protocol. *Rap1a*$^{-/-}$ mice were genotyped per a previously reported protocol (16). For *Rap1b*$^{-/-}$ mice, a new genotyping strategy was developed using the primers 5′-AGCCCTGGTAAGTCGTTCCT-3′ and 5′-GGGAAGCCCTTGGTTCTATC-3′. The HIV-1 Tg26 transgenic mouse model carries a gag/pol–deleted HIV-1 provirus (42) and develops a renal disease phenotypically identical to human HIVAN.

Histopathology and immunohistochemistry of mouse tissue. All kidneys were perfused in vivo with 4% PFA. For histological analysis, kidneys were left in PFA overnight and then embedded in paraffin. Sections were cut at 2 μm and stained with PAS. For IF, kidneys were fixed in PFA for 4 hours, transferred to 18% sucrose overnight, and then flash-frozen in OCT medium. For electron microscopy, samples were cut into 1-mm cubes and fixed overnight in 2.5% glutaraldehyde before being epoxy-embedded using standard techniques (JEOL 1011 electron microscope).

Podocyte cell culture. Generation and propagation of established conditionally immortalized podocyte cell lines has been described previously (39, 43). Briefly, podocytes were propagated on type I collagen–coated dishes at the permissive temperature (33°C) in RPMI supplemented with 10% FBS and 10 U/ml IFN-γ. To allow for differentiation, cells were shifted to the nonpermissive temperature (37°C) without IFN-γ.

Lentiviral production and infection. For overexpression of RAP1GAP, pLOC-GFP RAP1GAP was obtained from Open Biosystems. Infections were carried out at the permissive temperature in human podocytes, and then cells were immediately shifted to 37°C to allow for differentiation. Each experiment involved freshly infected cells. For RAP1GAP knockdown, lentiviral expression vectors carrying shRNAs were purchased from Sigma-Aldrich (Mission shRNA). The hairpin sequence that targets *Rap1gap* is CCTG-GTATTCTCGCTCAAGTA. Infections were done at the permissive temperature in mouse podocytes, and then stable cell lines were established by selection with puromycin. Stable RAP1GAP knockdown lines were grown at 37°C for at least 1 week prior to use in experiments. All lentiviral preparation and infections were performed as previously described (8).

Flow cytometry. Samples were collected using a FACSCanto II (BD) flow cytometer and analyzed using Flow Jo software (Tree Star).

Adhesion and migration assays. For adhesion assays, cells were trypsinized and plated onto 24-well plates precoated with laminin (10 μg/ml) or fibronectin (20 μg/ml) for 10 minutes. Nonadherent cells were removed by washing, and adherent cells were fixed in 3.7% formaldehyde and then stained with 0.1% crystal violet. After washing, the stain was eluted with 1% deoxycholic acid. Absorbances were read at 590 nm. All experiments were repeated in triplicate. For migration assays, differentiated podocytes were plated to confluence on collagen type I–coated 6-well plates. A scratch was created using a 200-μl sterile pipette, and then loosely adherent cells were removed by washing. Images were obtained at several fixed locations along the scratch at fixed time intervals.

RNA extraction and quantitative PCR. RNA was extracted from podocyte clones using RNeasy Purification Kit (Qiagen). Quantitative PCR was performed at Icahn School of Medicine at Mount Sinai Quantitative PCR Shared Research Facility. The facility uses an ABI PRISM 7900HT sequence detection systems using SYBR green. Primer sequences for murine *Rap1gap* were previously reported (34). Results were normalized to *Gapdh* and *Actb* expression.

Glomerular isolation and RAP1-GTP pulldowns. Glomeruli were isolated using a successive sieving approach using 3 screens with pore sizes of 180, 100, and 71 μm. Kidneys from 3 animals were pooled prior to sieving. To quantify RAP1-GTP, pulldowns were performed using a GST-tagged fusion protein, corresponding to amino acids 788–884 of human RalGDS–RAP-binding domain (RalGDS-RBD) bound to glutathione agarose (Millipore, 17-321).

Detachment and apoptosis assays. Murine podocytes were grown on 10-cm culture dishes at 37°C for at least 1 week. Fields of cells were marked, and cell number per field was counted to establish a baseline. Cells were treated with 25 μg/ml PAN, and then cell numbers were recounted for each field every 24 hours for a total of 96 hours. Blocking antibody Ha2/5 (dilution 1:25) was added to the media simultaneous to the addition of PAN and maintained for the duration of the experiment. An average of 5 fields in 2 individual experiments were averaged and analyzed statistically. Annexin V and propidium iodide assays were performed using Dead Cell Apoptosis Kit (Life Technologies) per the manufacturer's protocol. After exposure to PAN for a set time, detached podocytes were collected and then combined with adherent cells that were detached using trypsin. A combined cellular pellet was used for apoptosis quantification.

Statistics. All experiments were repeated 3 or more times unless otherwise indicated. Bar graphs represent combined results from all experiments. All data represent mean ± SEM. Statistical significance was determined by 2-tailed Student's *t* test. A *P* value less than 0.05 was considered significant.

Study approval. All mouse studies were approved by the IACUC at Icahn School of Medicine at Mount Sinai and followed NIH guidelines. Frozen sections from archived human biopsy material were obtained from Columbia University College of Physicians and Surgeons under an IRB-approved protocol entitled "Research with archival human renal biopsy tissues." All biopsies were clinically indicated, and only extra tissue not required for diagnostic purposes was permitted for research use; therefore, no patient informed consent was required.

Acknowledgments

This work was supported by NIDDK, NIH, grant 1R01DK084006 (to L. Kaufman) and NIH grant P01DK56492 (to P.E. Klotman).

Received for publication November 19, 2012, and accepted in revised form January 16, 2014.

Address correspondence to: Lewis Kaufman, Icahn School of Medicine at Mount Sinai, Division of Nephrology, Box 1243, One Gustave L Levy Place, New York, New York 10029, USA. Phone: 212.241.9431; Fax: 212.987.0389; E-mail: lewis.kaufman@mssm.edu.

1. Kriz W, Shirato I, Nagata M, LeHir M, Lemley KV. The podocyte's response to stress: the enigma of foot process effacement. *Am J Physiol Renal Physiol*. 2013;304(4):F333–F347.
2. Kooistra MR, Dube N, Bos JL. Rap1: a key regulator in cell-cell junction formation. *J Cell Sci*. 2007; 120(pt 1):17–22.
3. Bos JL, Rehmann H, Wittinghofer A. GEFs and GAPs: critical elements in the control of small G proteins. *Cell*. 2007;129(5):865–877.
4. Tsygankova OM, et al. Downregulation of Rap1GAP in human tumor cells alters cell/matrix and cell/cell adhesion. *Mol Cell Biol*. 2010;30(13):3262–3274.
5. Zuo H, et al. Downregulation of Rap1GAP through epigenetic silencing and loss of heterozygosity promotes invasion and progression of thyroid tumors. *Cancer Res*. 2010;70(4):1389–1397.
6. Zheng H, Gao L, Feng Y, Yuan L, Zhao H, Cornelius LA. Down-regulation of Rap1GAP via promoter hypermethylation promotes melanoma cell proliferation, survival, and migration. *Cancer Res*. 2009; 69(2):449–457.
7. Barisoni L, Kriz W, Mundel P, D'Agati V. The dysregulated podocyte phenotype: a novel concept in the pathogenesis of collapsing idiopathic focal segmental glomerulosclerosis and HIV-associated nephropathy. *J Am Soc Nephrol*. 1999;10(1):51–61.
8. Husain M, et al. HIV-1 Nef induces proliferation and anchorage-independent growth in podocytes. *J Am Soc Nephrol*. 2002;13(7):1806–1815.
9. Gharavi A, Oller S, Bruggeman L, Lifton R, Klotman P. Genetic background modifies the development of renal disease in HIV-1 transgenic mice. *J Amer Soc Nephrol*. 1999;10:404A.
10. Wyatt CM, Meliambro K, Klotman PE. Recent progress in HIV-associated nephropathy. *Annu Rev Med*. 2012;63:147–159.
11. Gharavi AG, et al. Mapping a locus for susceptibility to HIV-1-associated nephropathy to mouse chromosome 3. *Proc Natl Acad Sci U S A*. 2004; 101(8):2488–2493.
12. Hodgin JB, et al. A molecular profile of focal segmental glomerulosclerosis from formalin-fixed, paraffin-embedded tissue. *Am J Pathol*. 2010; 177(4):1674–1686.
13. Bennett MR, Czech KA, Arend LJ, Witte DP, Devarajan P, Potter SS. Laser capture microdissection-microarray analysis of focal segmental glomerulosclerosis glomeruli. *Nephron Exp Nephrol*. 2007; 107(1):e30–40.
14. Li Y, et al. Rap1a null mice have altered myeloid cell functions suggesting distinct roles for the closely related Rap1a and 1b proteins. *J Immunol*. 2007; 179(12):8322–8331.
15. Chrzanowska-Wodnicka M, Kraus AE, Gale D, White GC, White GC 2nd, Vansluys J. Defective angiogenesis, endothelial migration, proliferation, and MAPK signaling in Rap1b-deficient mice. *Blood*. 2008;111(5):2647–2656.
16. Pan BX, Vautier F, Ito W, Bolshakov VY, Morozov A. Enhanced cortico-amygdala efficacy and suppressed fear in absence of Rap1. *J Neurosci*. 2008; 28(9):2089–2098.
17. Shih NY, et al. Congenital nephrotic syndrome in mice lacking CD2-associated protein. *Science*. 1999; 286(5438):312–315.
18. Roselli S, et al. Early glomerular filtration defect and severe renal disease in podocin-deficient mice. *Mol Cell Biol*. 2004;24(2):550–560.
19. Kim C, Ye F, Ginsberg MH. Regulation of integrin activation. *Annu Rev Cell Dev Biol*. 2011;27:321–345.
20. Boettner B, Van Aelst L. Control of cell adhesion dynamics by Rap1 signaling. *Curr Opin Cell Biol*. 2009; 21(5):684–693.
21. Pozzi A, et al. β1 integrin expression by podocytes

is required to maintain glomerular structural integrity. *Dev Biol*. 2008;316(2):288–301.
22. Kanasaki K, et al. Integrin β1-mediated matrix assembly and signaling are critical for the normal development and function of the kidney glomerulus. *Dev Biol*. 2008;313(2):584–593.
23. Schwartz MA, Assoian RK. Integrins and cell proliferation: regulation of cyclin-dependent kinases via cytoplasmic signaling pathways. *J Cell Sci*. 2001; 114(pt 14):2553–2560.
24. de Bruyn KM, Rangarajan S, Reedquist KA, Figdor CG, Bos JL. The small GTPase Rap1 is required for Mn(2+)- and antibody-induced LFA-1- and VLA-4-mediated cell adhesion. *J Biol Chem*. 2002; 277(33):29468–29476.
25. Choma DP, Pumiglia K, DiPersio CM. Integrin α3β1 directs the stabilization of a polarized lamellipodium in epithelial cells through activation of Rac1. *J Cell Sci*. 2004;117(pt 17):3947–3959.
26. Chen CA, Hwang JC, Guh JY, Chang JM, Lai YH, Chen HC. Reduced podocyte expression of α3β1 integrins and podocyte depletion in patients with primary focal segmental glomerulosclerosis and chronic PAN-treated rats. *J Lab Clin Med*. 2006;147(2):74–82.
27. Bazzoni G, Ma L, Blue ML, Hemler ME. Divalent cations and ligands induce conformational changes that are highly divergent among β1 integrins. *J Biol Chem*. 1998;273(12):6670–6678.
28. Maslov S, Sneppen K. Specificity and stability in topology of protein networks. *Science*. 2002; 296(5569):910–913.
29. Schroder AR, Shinn P, Chen H, Berry C, Ecker JR, Bushman F. HIV-1 integration in the human genome favors active genes and local hotspots. *Cell*. 2002;110(4):521–529.
30. Mitchell RS, et al. Retroviral DNA integration: ASLV, HIV, and MLV show distinct target site preferences. *PLoS Biol*. 2004;2(8):E234.
31. Bushman F, et al. Genome-wide analysis of retroviral DNA integration. *Nat Rev Microbiol*. 2005; 3(11):848–858.
32. Ptak RG, et al. Cataloguing the HIV type 1 human protein interaction network. *AIDS Res Hum Retroviruses*. 2008;24(12):1497–1502.
33. Felice B, et al. Transcription factor binding sites are genetic determinants of retroviral integration in the human genome. *PLoS One*. 2009;4(2):e4571.
34. Niola F, et al. Id proteins synchronize stemness and anchorage to the niche of neural stem cells. *Nat Cell Biol*. 2012;14(5):477–487.
35. Su L, et al. AF-6 controls integrin-mediated cell adhesion by regulating Rap1 activation through the specific recruitment of Rap1GTP and SPA-1. *J Biol Chem*. 2003;278(17):15232–15238.
36. Zhang L, et al. Identification of a putative tumor suppressor gene Rap1GAP in pancreatic cancer. *Cancer Res*. 2006;66(2):898–906.
37. Duchniewicz M, Zemojtel T, Kolanczyk M, Grossmann S, Scheele JS, Zwartkruis FJ. Rap1A-deficient T and B cells show impaired integrin-mediated cell adhesion. *Mol Cell Biol*. 2006;26(2):643–653.
38. Chrzanowska-Wodnicka M, Smyth SS, Schoenwaelder SM, Fischer TH, White GC. Rap1b is required for normal platelet function and hemostasis in mice. *J Clin Invest*. 2005;115(3):680–687.
39. Saleem MA, et al. A conditionally immortalized human podocyte cell line demonstrating nephrin and podocin expression. *J Am Soc Nephrol*. 2002; 13(3):630–638.
40. Ciuffi A, Barr SD. Identification of HIV integration sites in infected host genomic DNA. *Methods*. 2011;53(1):39–46.
41. Kaufman L, et al. Up-regulation of the homophilic adhesion molecule sidekick-1 in podocytes contributes to glomerulosclerosis. *J Biol Chem*. 2010; 285(33):25677–25685.
42. Kopp JB, et al. Progressive glomerulosclerosis and enhanced renal accumulation of basement membrane components in mice transgenic for human immunodeficiency virus type 1 genes. *Proc Natl Acad Sci U S A*. 1992;89(5):1577–1581.
43. Mundel P, et al. Rearrangements of the cytoskeleton and cell contacts induce process formation during differentiation of conditionally immortalized mouse podocyte cell lines. *Exp Cell Res*. 1997; 236(1):248–258.